

This is the **accepted version** of the journal article:

Montagut, Ana Maria; Granados Toda, Albert; Lazurko, Caitlin; [et al.]. «Triazine mediated covalent antibiotic grafting on cotton fabrics as a modular approach for developing antimicrobial barriers». *Cellulose*, Vol. 26, Issue 12 (August 2019), p. 7495-7505. DOI 10.1007/s10570-019-02584-w

This version is available at <https://ddd.uab.cat/record/273777>

under the terms of the  ^{IN} COPYRIGHT license

1 **Triazine Mediated Covalent Antibiotic Grafting on Cotton Fabrics as a**
2 **Modular Approach for Developing Antimicrobial Barriers**

3
4 **Ana Maria Montagut,^a Albert Granados,^a Caitlin Lazurko,^{b,c} Antony El-Khoury,^b Erik**
5 **J. Suuronen,^b Emilio I. Alarcon,^{b,c,*} Rosa María Sebastián,^{a,*} Adelina Vallribera^{a,*}**

6 *(a) Department of Chemistry and Centro de Innovación en Química (ORFEO-CINQA),*
7 *Universitat Autònoma de Barcelona, Campus UAB, 08193-Cerdanyola del Vallès, Barcelona,*
8 *Spain.*

9 *(b) Division of Cardiac Surgery, University of Ottawa Heart Institute, Ottawa, Canada, 40*
10 *Ruskin Street, Ottawa, Ontario K1Y 4W7, Canada*

11 *(c) Department of Biochemistry, Microbiology, and Immunology, Faculty of Medicine,*
12 *University of Ottawa, 451 Smyth Road, Ottawa, Ontario K1H 8M5, Canada*

13
14 **Dr. Ana Maria Montagut:** anamaria.montagut1@gmail.com

15 **Dr. Albert Granados:** albert.granados@uab.es

16 **Caitlin Lazurko:** clazu027@uottawa.ca

17 **Antony El-Khoury:** aelkh065@uottawa.ca

18 **Dr. Erik J. Suuronen:** esuuronen@ottawaheart.ca

19 **Corresponding to:**

20 **Dr. Emilio I. Alarcon:** ealarcon@ottawaheart.ca

21 **Dr. Rosa María Sebastián:** rosamaria.sebastian@uab.es

22 **Prof. Adelina Vallribera;** adelina.vallribera@uab.es

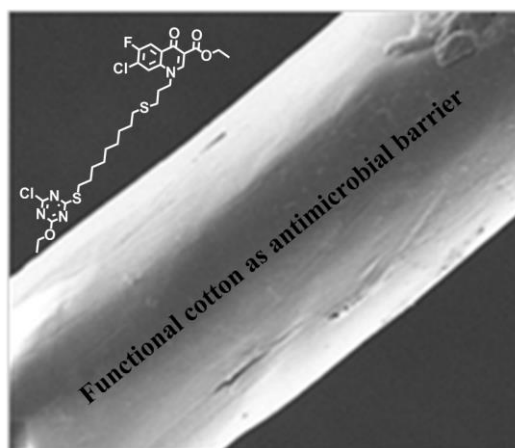
23
24 **Abstract**

25 New antimicrobial textiles were prepared through direct chemical linkage of bioactive
26 molecules eugenol and fluoroquinolone derivatives, onto the surface of cotton fabrics. The
27 attachment through a triazine moiety minimizes the leaching of the antimicrobial molecule into
28 the surroundings of the material. Bacterial efficacy against *Staphylococcus aureus* and
29 *Pseudomonas aeruginosa* was studied. The treated textile with fluoroquinolone demonstrated

30 bacteriostatic antimicrobial effects having a tendency to decrease the population of *S. aureus* in
31 the planktonic form. A significant effect was also observed in the prevention of *S. aureus*
32 biofilm formation and in its ability to kill bacteria within a preformed biofilm. Eugenol-
33 modified fabric was also active in the process of eradicating preformed *P. aeruginosa* biofilms.
34 Further, *in vitro* assays using human dermal fibroblast cells indicate no effects on cell
35 proliferation and viability, and *in vivo* tests in a murine skin wound model showed no increase
36 of IL-6 for full-thickness wounds that were in contact with the fabrics.

37

38 **Keywords:** microbicidal; cotton fabrics; covalent functionalization; fluoroquinolone;
39 biocompatibility; biofilm destruction



40

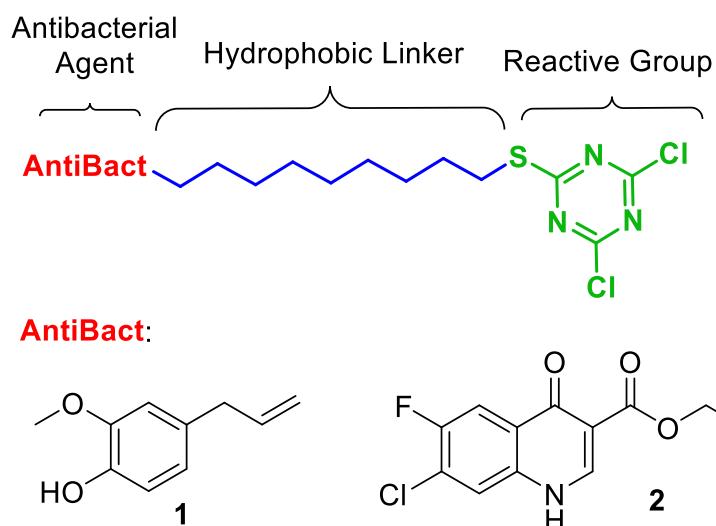
41 1. Introduction

42 The incorporation of bioactive molecules into the structure of textiles has gained increasing
43 attention in the last decade (Shahidi and Wiener 2012, Pinho et. al. 2010, Koh and Hong 2014,
44 Salama et. al. 2015). Antimicrobials are one of the most frequently used agents in bioactive
45 textiles, since they effectively minimize the risk of microbial infection (Klivanov 2007, Ristić
46 et. al. 2011, Hong 2014, Shahidi et. al. 2014). The bioactive agent may be either covalently
47 bound or physio-adsorbed to the textile fiber. In the latter case, there is a burst release of the
48 bioactive agent, which is detrimental for long term protection of the wound. Thus, chemical
49 anchoring of bioactive molecule improves the lifetime of the material and also prevents the
50 leaching of bioactive substances out of the textile, minimizing, for example, the risk of
51 developing antibiotic resistant bacterial strains.

52 Naturally occurring fibrous structures, like cellulose, are particularly suitable for medical
53 applications due to their mechanical properties, high hydrophilicity, and capability to absorb
54 biofluids (*e.g.*, wound oozing). Cotton has been widely used for textiles because of its
55 breathability, softness, and biodegradability (Xu et. al. 2010, Koga et. al. 2010). Thus, having
56 the surface of cotton functionalized with antimicrobial agents will open the door to develop
57 novel materials for controlling topical infections. Some strategies for bonding active substances
58 to cellulosic fibers have been reported (Simoncic and Tomsic 2010), including antimicrobial
59 agents such as quaternary ammonium salts (QAS) derivatives (Lin et. al. 2003, Hsu and
60 Klibanov 2011, Gutarowska et. al. 2013, Song and Baney 2016), *N*-halamine derivatives (Sun
61 et. al. 2001), and chitosan (Öktem 2003, Abramiuc et. al. 2013, Gargoubi et. al. 2016). Such
62 methodologies are rather complex in nature, including for examples the use of polycarboxylic
63 acids to chemically crosslink the chitosan to cellulose (Öktem 2003). Thus, there is still a need
64 to develop synthetic routes for producing materials grafted with antimicrobial agents for wound
65 dressing. For covalent anchoring on the textiles, cyanuric chloride, highly reactive towards
66 nucleophiles through an aromatic nucleophilic substitution and of low cost, was selected as
67 reactive group (Figure 1). This triazine unit has been previously used by our group for the
68 dyeing of textiles by grafting. Triarylmethane (Montagut et. al. 2017), anthraquinone (Salabert
69 et. al. 2015) and azo (Soler et. al. 2011) fluorinated dyes were anchored on textiles using a
70 triazine moiety to obtain artificial repellent cotton fibers. Recently, other groups have used
71 triazine to prepare covalently modified functional cotton fabrics, as for example triazine based
72 reactive dyes for wool fabric ink printing (Yang et. al. 2018); monochlorotriazine
73 triethylphosphite guanidine for flame retardant cotton fabrics (Dong et. al. 2018); and *N*-
74 halamine triazine salts derivatives for antibacterial cellulose (Jiang et. al. 2019).

75 In this work, we present a novel approach for covalently tethering of antibiotics onto cotton
76 fabrics through a nucleophilic aromatic substitution on a triazine moiety. The antibiotics were
77 first modified with a linker (Figure 1). The long hydrocarbon chain in the linker will increase
78 the hydrophobicity and the microbicide potency (Liu et. al. 2013) and will decrease the steric
79 hindrance for the subsequent grafting onto the cotton surface. The ideal strategy should preserve
80 the pharmacological efficacy of the active substance and be versatile to allow the anchoring of
81 other active substances.

82



83

84 **Fig. 1** Representation of our novel anchoring system for grafting antimicrobial agents to

85 textiles. Structure of antibiotics **1** and **2**.

86 Two different families of antibiotics were selected to be grafted onto cotton fabrics: (i) 2-
 87 methoxy-4-(prop-2-en-1-yl)phenol (Eugenol, **1**) (Kalemba and Kunicka 2003, Rojo et. al.
 88 2008), and (ii) ethyl 7-chloro-6-fluoro-4-oxo-1,4-dihydroquinoline-3-carboxylate
 89 (fluoroquinolone, **2**) (Koga et. al. 1980) (Figure 1). Eugenol, **1**, was first chosen due to its
 90 known antibacterial properties. It has been reported that **1** inhibits the growth of a range of
 91 microorganisms such as *Escherichia coli* (Blaszyk and Holley 1998), *Penicillium citrinium*
 92 (Vazquez et. al. 2001) and human herpes virus in vitro (Benecia and Courreges 2000). In
 93 medical field is mainly used in dentistry as a root canal sealer (Rojo et. al. 2008). Next, we
 94 selected quinolones another well-known family of antibiotics, and specifically one that is highly
 95 active the fluoroquinolone **2** (Leyva and Leyva 2008, Aldred et. al. 2014).

96 After the covalent tethering of Eugenol and fluoroquinolone to the surface of cotton textiles the
 97 *in vitro* antibacterial activity and cell toxicity of these functionalized fabrics were assessed
 98 together with *in vivo* assays in a full-thickness wound model in mice.

99

100 **2. Experimental section**

101 **2.1. Materials**

102 Eugenol, glycerol, diethyl ether, cyanuric chloride, *N,N*-Diisopropylethylamine, anhydrous
 103 tetrahydrofuran, anhydrous sodium sulfate, anhydrous acetone, sodium hydroxide, hexane,
 104 lysogeny (LB) broth, lysogeny (LB) broth agar, hydrochloric acid, acetic acid, tryptone, yeast

105 extract, DMSO-*d*₆, CDCl₃, potassium carbonate, and sodium chloride were purchased from
106 Sigma Aldrich. All solutions were prepared using Milli-Q water. All cell culture media and
107 reagents were purchased from Thermo Fisher Scientific Gibco unless otherwise specified.

108

109 ***2.2. General procedure for the thiol–ene reactions***

110 In a 25 mL round bottom flask (see supporting information for details on structures), eugenol,
111 **1**, (0.50 g, 3.0 mmol, 1 eq.), **2** (1.3 mL, 9.0 mmol, 3 eq.) and 6 mL of glycerol were added. The
112 mixture was warmed to 80°C and stirred for 3h. Extractions were done using Et₂O and water.
113 Then, the organics were evaporated. The resulting crude product was purified by a
114 chromatographic column with an eluent solution of 2:1 (Hex:Et₂O), affording 0.76 g of **3** as a
115 white solid (85% yield) and 0.13 g of **4** (8% yield).

116

117 ***2.3. General procedure for the reaction with cyanuril chloride. Example of preparation of 9***

118 In a 100 mL Schlenk flask under Ar atmosphere, cyanuric chloride (0.28 g, 1.4 mmol, 1.3 eq.),
119 DIPEA (0.3 mL, 1.8 mmol, 1.7 eq.), and 30 mL of anhydrous THF were added. The mixture
120 was cooled to -20°C. Next, a solution of 4-(3-((9-mercaptononyl)thio)propyl)-2-
121 methoxyphenol, **3**, (0.38 g, 1.1 mmol, 1 eq.) and 60 mL of anhydrous THF were added
122 dropwise. The addition time was 5 h and the reaction was stirred for 1 h more. Afterwards, the
123 THF was dried with anhydrous NaSO₄ and evaporated. The residue was purified by a
124 chromatographic column using Hex:Et₂O as an eluent following a gradient from 3:1 to 1:1. The
125 chromatographic column made long tails of the final product. A white solid was obtained,
126 corresponding to **9**, 0.14 g, 36% yield.

127

128 ***2.4. General procedure for the attachment of the functional antimicrobial molecule on the*** 129 ***cotton surface***

130 A piece of cotton fabric (3 x 3 mm) was washed in a solution of soap and K₂CO₃ under reflux
131 for 3 h. The cotton fabric was then dried and placed in a 1 M NaOH solution for 1 h. Next, the
132 fabric was washed with anhydrous acetone and dried. Finally, the fabric was placed in a multi-
133 reactor tube with a 0.23% w/v solution of the antibiotic molecule that was to be anchored to the
134 fabric (the antibiotic derivative) in 10 mL of anhydrous THF. The set up was left under reflux
135 for 3 days.

136

137 ***2.5. Characterization techniques***

138 Melting points were measured in a *bloc Kofler* apparatus from *Reichert* or in a *B-545* apparatus
139 from *Büchi* and are uncorrected. ¹H- (250 MHz) and ¹³C- (62.5 MHz) NMR (Nuclear Magnetic
140 Ressonance) spectra were obtained using a *Brucker AC-250* spectrometer. ¹H- (360 MHz) and
141 ¹³C- (90 MHz) NMR spectra were obtained using a *Brucker Avance 360* spectrometer. All
142 chemical shifts are given in δ (ppm). ¹H-NMR and ¹³C NMR are refereed with respect to TMS.
143 IR (Infrared) spectra (neat) were performed in a *Bruker Tensor 27* using an ATR (Attenuated
144 Total Reflectance) *Golden Gate* modulus provided with a diamond tip. All data are given in
145 wave number ν and cm^{-1} . HR-ESI-MS (High Resolution-Electrospray Ionization Mass
146 Spectrometry) experiments were performed using a *MicroTof-Q* from *Bruker daltronics* in
147 either positive or negative ionization mode.

148

149 **2.6. Antimicrobial assays**

150 The antimicrobial properties of the fabrics were tested against *Staphylococcus aureus* (ATCC
151 25923) and *Pseudomonas aeruginosa* (PAO1). Bacterial suspensions were freshly prepared by
152 diluting overnight cultures in LB broth. Overnight cultures were prepared by resuspending one
153 colony in 2.0 mL of LB agar and culturing in an orbital shaker for 18 h.

154 The antimicrobial effects of the fabrics were tested by incubating a 3 x 3 mm piece of
155 antimicrobial fabric (**Fabric A** and **Fabric B**) in bacterial suspensions of 10^7 CFU/mL at 37 °C
156 for 18 h. The number of surviving colonies was quantified by first diluting the treated solution
157 to 10^4 and 10^5 CFU/mL, and then plating 10 μL of the diluted solution on an agar plate. The
158 agar plates were then incubated at 37 °C for 14 h, and the number of colonies was counted.

159

160 **2.7. Biocompatibility and proliferation assay**

161 To determine the biocompatibility of the fabrics, 5,000 human skin dermal fibroblasts/well were
162 cultured in DMEM (Dulbecco's Modified Eagle Medium) in a 96-well plate. The cells were
163 cultured for 2 days at 37 °C with 5% CO_2 . Next, a 3 x 3 mm piece of fabric was added to each
164 well and cells were incubated for up to 15 days. An MTS assay was performed to determine the
165 metabolic activity of the cells following the manufacturer's protocol (CellTiter 96® Aqueous
166 One Solution Cell Proliferation Assay, Promega). Briefly, 20 μL of the MTS solution was added
167 to each well and incubated for 3 h. Then the absorbance of each well was measured at 490 nm.

168

169 **2.8. In vivo IL-6 concentration**

170 *Animals*

171 All animal studies were conducted with ethical approval from the University of Ottawa Animal
172 Care Committee and in compliance with the National Institutes of Health Guide for the Use of
173 Laboratory Animals. Female C57Bl/6 mice purchased from Charles River Laboratories were
174 used for all experiments.

175 Eight week old female C57 mice were anesthetized with 2.5% isoflurane through a nose cone
176 inhaler. Their backs were shaved and washed with 70% ethanol and two dorsal full thickness
177 skin wounds were made with a circular punch, 6 mm in diameter. The left wound was used as
178 a control while the right wound received the treatment, consisting of a 0.5 cm x 0.5 cm piece
179 of fabric placed in the wound bed. The wounds were kept open with a silicone disk covered
180 with Tegaderm™ and secured with 5 sutures. All animals were monitored for signs of
181 inflammation, and pain was managed by Buprenorphine administered post-surgery. The
182 animals were sacrificed 24h after the treatment. The wound area was collected and frozen at -
183 80°C and the IL-6 concentration was measured by an enzyme-linked immunosorbent assay
184 (ELISA; see below).

185 *IL-6 concentration*

186 The concentration of pro-inflammatory cytokine IL-6 was assessed in homogenized skin tissue
187 harvested from the wound area after 24 hours of treatment using a mouse IL-6 ELISA kit
188 (Thermo Fisher Scientific). Samples were homogenized in homogenization buffer (100 mM
189 Tris, pH 7.4, 150 mM NaCl, 1 mM EGTA, 1 mM EDTA, 1% Triton-X, 0.5% sodium
190 deoxycholate, 1 mM PMSF, 1x Halt™ Protease and Phosphatase Inhibitor Cocktail (Thermo
191 Fisher Scientific)) using 0.5 mm zirconium silicate beads (Next Advance) for 15 minutes in a
192 Bullet Blender Tissue Homogenizer (Next Advance) followed by centrifugation at 10,000 xg
193 for 10 minutes. The supernatant was then frozen at -80 °C until use. All samples were
194 normalized to a starting concentration of 1 mg/mL of total protein, determined by bicinchoninic
195 acid assay (BCA, Thermo Fisher scientific).

196 The ELISA assay was completed as per the manufacturer's instructions (see
197 https://tools.thermofisher.com/content/sfs/manuals/KMC0061_KMC0062_Ms_IL6.pdf).

198 Briefly, a serial dilution of freshly prepared IL-6 standard (10,000 pg/mL) was completed to
199 create a working range of 0 – 500 pg/mL. For this solid-phase sandwich ELISA, 100 µL of
200 samples and standards were added to wells pre-layered with designated 1^o antibodies and
201 incubated for 2 h at room temperature. The plate was then washed 4 times with wash buffer.
202 Next, 100 µL of mouse IL-6 biotin conjugate solution was added to the wells and incubated for
203 30 min at room temperature. The plate was then washed 4 times with wash buffer. Then 100
204 µL of streptavidin-HRP was added to the wells and incubated for 30 min at room temperature.

205 The plate was then washed 4 times with wash buffer. Next, 100 μ L of chromogen was added to
206 the wells and incubated for 30 min at room temperature in the dark. The reaction was halted by
207 the addition of 100 μ L of stop solution. The absorbance was then read at 450 nm. Controls were
208 prepared with PBS without biotin conjugate and streptavidin-HRP. The concentration of IL-6
209 in samples was determined using a standard curve generated from the standard IL-6 solutions.

210

211 **2.9. Anti-biofilm assay**

212 *Pseudomonas aeruginosa* PAO1 biofilms were grown by incubating a bacterial suspension (10^7
213 cfu/ml) in M63 medium broth on glass surfaces arranged into the wells of a 12-well plate for
214 6h at 37 °C. Once the biofilm was visibly formed, the remaining liquid was aspirated, and a
215 piece of each fabric was placed on the formed biofilm and incubated for 12h at 37 °C. Triplicate
216 experiments were completed for each treatment. The fabrics were then removed, and the biofilm
217 were visualized using crystal violet stain.

218 Antibiotic leaching was testing by incubating a 3 x 3 mm square piece of Fabric A with 100 μ l
219 of 25% LB broth overnight. The fabric was the removed and 10^7 CFU/mL of *P. aeruginosa*
220 strain PAO1 was added to the solution and incubated at 37 °C for 18 h. Bacterial growth was
221 monitored to determine if leaching has occurred.

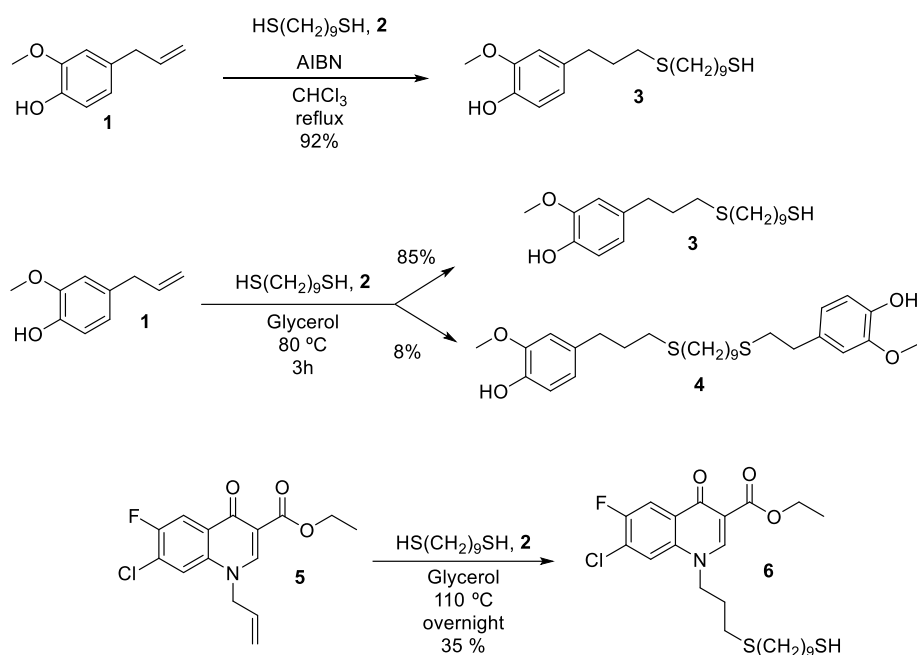
222

223 **3. Results and discussion**

224 **3.1. Preparation of AntiBact-S-(CH₂)₉-SH**

225 Given that the functional groups of antibiotics may play a crucial rule in their bioactivity, the
226 point of attachment of the linker HS-(CH₂)₉-SH was carefully selected (**Scheme 1**). Thus, the
227 double bound present on eugenol structure was deliberately picked to attach the linker. We
228 tested several common thiol-ene coupling protocols between **1** and 1,9-nonandithiol.
229 Moreover, we decided to incorporate a vinyl group on the fluoroquinolone that should allow
230 the covalent attachment of the linker without affecting the functional groups involved in the
231 bioactivity. Thus, derivative **5** was prepared following a methodology previously described by
232 Koga (Koga et. al. 1980). Using the chemical anchoring system depicted in **Scheme 1**, we first
233 linked both antibiotics (**1** and **5**) to a thioether hydrophobic arm to form the derivative of the
234 formula AntiBact-S-(CH₂)₉-SH. The long hydrocarbon chain in the linker increases the
235 hydrophobicity and the microbicide potency by acting as a barrier and controlling
236 microorganism infiltration (Liu et. al. 2013). Furthermore, decreases the steric hindrance for
237 subsequent chemical modifications. Then, the thiol group at the end of the AntiBact-S-(CH₂)₉-
238 SH will be used to link the compound to the reactive group (**Figure 1**).

239 Both UV- and thermally-induced methods of the thiol-ene reactions were studied, with the best
240 results achieved under thermal activation with AIBN as the radical source (Dondoni 2008). An
241 excess of dithiol was used to minimize side reactions, giving a 92% yield of thioether **3** (**Scheme**
242 **1**). The high resolution mass-spectroscopy (HRMS (ESI⁺)) analysis (m/z [M+H]⁺ = 379.1733,
243 Figure S6) and ¹H NMR of **3** (Figure S2) confirmed its structure. The signals present in the ¹H
244 NMR of **3** were consistent with the presence of different methylene groups, among them CH₂-
245 S-CH₂ and CH₂SH were identified (absorption at δ = 2.46-2.58). No signals corresponding to
246 olefinic protons were detected. In addition, a multiplet at δ = 1.25-1.44 confirmed the presence
247 of the SH group (see SI). However, under the optimized conditions, fluoroquinolone derivative
248 **5** bearing a vinyl group (**Scheme 1**) did not react. Next, following the procedure from Perin *et*
249 *al.*, we used a catalyst-free synthesis for linear thioethers (Lenardão et. al. 2013). First, eugenol,
250 **1**, was reacted with nonane-1,9-dithiol, **2**, in glycerol at 80°C (85% yield, **Scheme 1**). In this
251 experiment, compound **4** was also isolated in 8% yield; its characterization confirmed the
252 presence of the dithiol-bridged dimer. The HRMS (ESI⁺) analysis (m/z [M+H]⁺ = 543.2573,
253 Figure S10) and ¹H NMR spectrum of **4** confirmed its structure. In the ¹H NMR spectrum the
254 signals corresponding to the 10 methylene central protons of the bridge –
255 S(CH₂)₂(CH₂)₁₀(CH₂)₂S were observed (δ = 1.30-1.38 ppm, Figure S8). The same conditions
256 were applied to obtain the thiol-bearing fluoroquinolone ester **6**. The reaction of **5** with 1,9-
257 nonandithiol gave a moderate 35% yield of **6** (**Scheme 1**). The HRMS (ESI⁺) analysis was
258 recorded for compound **6** (m/z [M+Na]⁺ = 524.1459, Figure S18). Its ¹H NMR spectrum (Figure
259 S15) revealed a complex absorption at δ = 2.46-2.66 ppm characteristic of the methylene groups
260 present in CH₂-S-CH₂ and CH₂SH and in addition, a multiplete at δ = 1.20-1.44 ppm
261 corresponding to the SH free group was also observed.



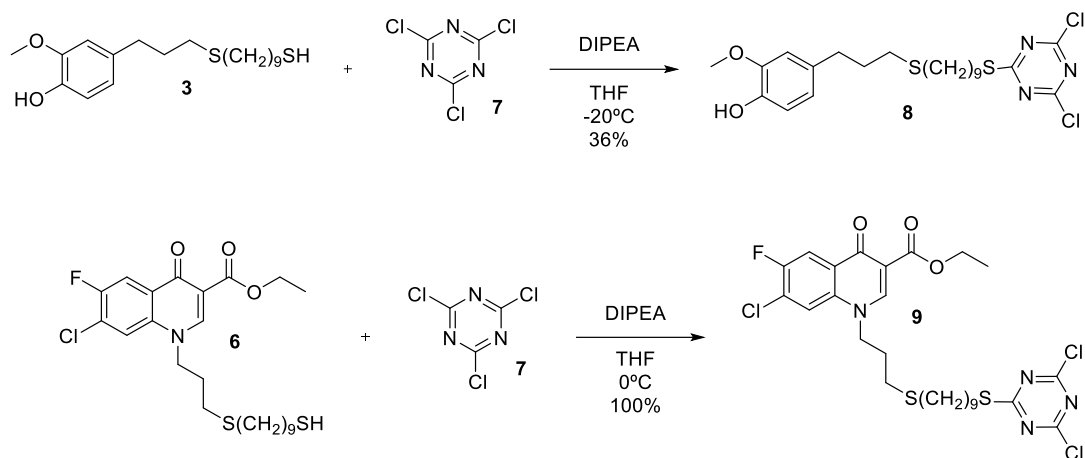
262

263

Scheme 1. Synthesis of AntiBact-S-(CH₂)₉-SH

264 In the next step, the AntiBact-S-(CH₂)₉-SH compounds were attached to a reactive group to
 265 functionalize the antimicrobial molecules (**Figure 1**). Cyanuric chloride, **7**, (2,4,6-trichloro-
 266 1,3,5-triazine) was reacted with the thiol group of the AntiBact-S-(CH₂)₉-SH through an
 267 aromatic nucleophilic substitution (**Scheme 2**). This reaction was carried out in the presence of
 268 the weak and bulky base *N,N*-diisopropylethylamine (DIPEA) in tetrahydrofuran. The coupling
 269 reaction was completed at low temperature to avoid multiple substitutions on **7**, which has three
 270 available sites for substitution. A mono-substituted cyanuric chloride is preferred to avoid steric
 271 hindrance in the subsequent reaction of the reactive antibacterial molecule with the cellulose
 272 fabric. Moreover, tri-substitution would prevent the bonding of the functionalized antimicrobial
 273 molecule to the cellulose, since all the reactive sites of **7** would already be used. After some
 274 experimentation, reaction of **3** with **7** (1.25 equiv.) in the presence of 1.65 equiv. of DIPEA was
 275 carried out at -20°C (**Scheme 2**). In these conditions, di- and tri-substitution reactions and the
 276 addition of the phenol to the cyanuric chloride were minimized, obtaining **8** in 36% yield. The
 277 ¹H NMR spectrum of **8** (Figure S20) showed different types of CH₂ groups, the most relevant
 278 being the triplet signal at δ = 3.18 ppm (CH₂-S-triazine). The HRMS (ESI)⁺ m/z = 526.1112
 279 corresponded to [M+Na]⁺ (Figure S22). The ¹³C NMR spectrum (Figure S21) presented a signal
 280 at δ = 170.0 ppm confirming the C_{ar}-Cl bond of the triazine moiety. In contrast of the moderate
 281 yield obtained in the synthesis of **8**, the reaction for compound **6** was quantitative at 0°C
 282 (**Scheme 2**). The ¹H NMR spectrum (Figure S24) of **9** showed a triplet signal at δ = 3.13 ppm
 283 (CH₂-S-triazine) and the ¹³C NMR spectrum (Figure 25) presented a signal at δ = 169.7

284 confirming the C_{ar}-Cl bond of the triazine moiety (see SI). In addition, the HRMS (ESI)⁺ m/z =
285 671.0846 was consistent to [M+Na]⁺ confirming the structure (figure S26).



Scheme 2. Synthesis of functional antimicrobial molecules

288 3.2. Preparation of the functionalized cotton fabrics

289 Once the functional antimicrobial molecules had been prepared, we proceeded to modify the
290 cotton surface. First, each piece of cotton (piece of 3x3 cm) was washed under reflux in a water
291 solution of soap and potassium carbonate for 3h. Then the cotton fabric was dried and soaked
292 in a 1.0 M NaOH solution for 1h. Next, each piece of cotton fabric was washed with anhydrous
293 acetone, dried, and added to a multi-reactor tube containing a solution 0.23% w/v of **8** or **9** in
294 anhydrous THF. The mixture was left under reflux for a period of 3 days. After the anchorage
295 process the fabrics were rinsed with THF and acetone. The obtained organic solvents were pure
296 despite the high solubility of the functional antimicrobial molecules in both acetone and THF,
297 proving the stability of the linkage of **8** (**Fabric A**) and **9** (**Fabric B**) through the covalent bond
298 to the cotton surface (**Figure 2**).

299 SEM is the most widely used tool for morphological analysis. SEM micrographs of untreated
300 cotton fabric, **Fabric A** and **Fabric B** were performed (**Figure 3**). After covalent anchoring of
301 **8** and **9** the surface morphology has slightly changed and more significant differences are
302 observed for **Fabric B**.

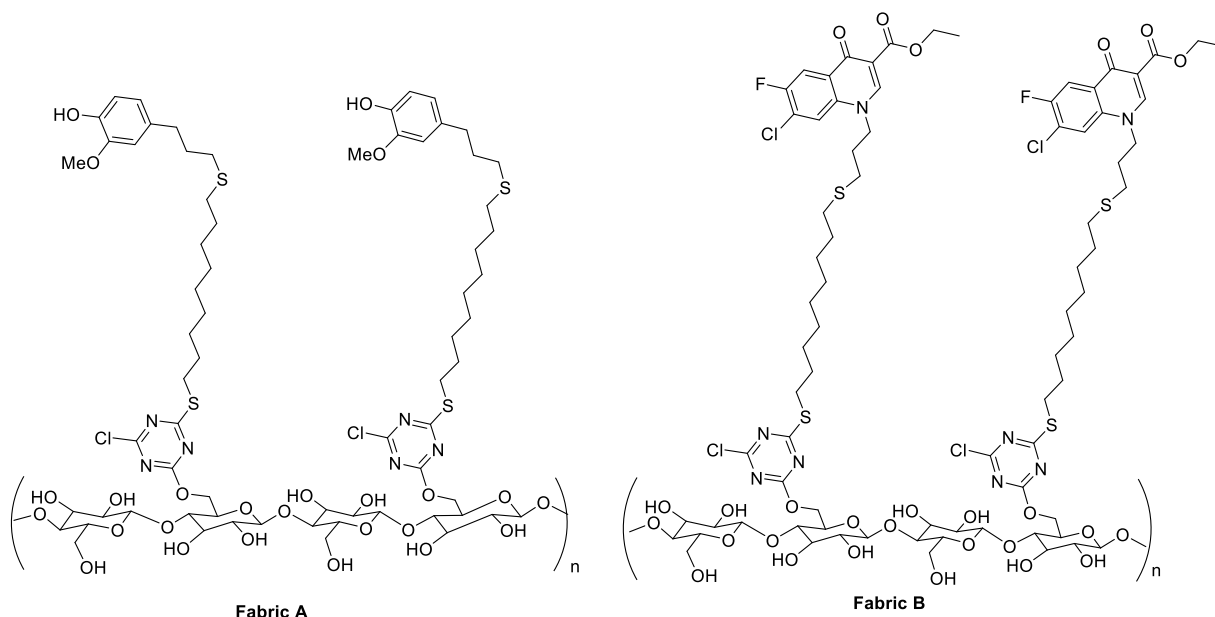


Fig. 2 Proposed structures for functionalized cotton fabrics.

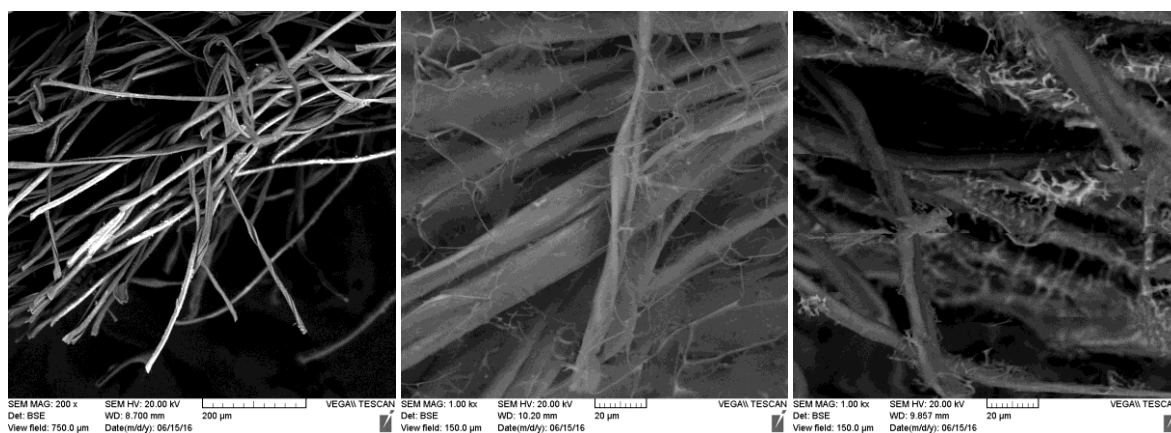
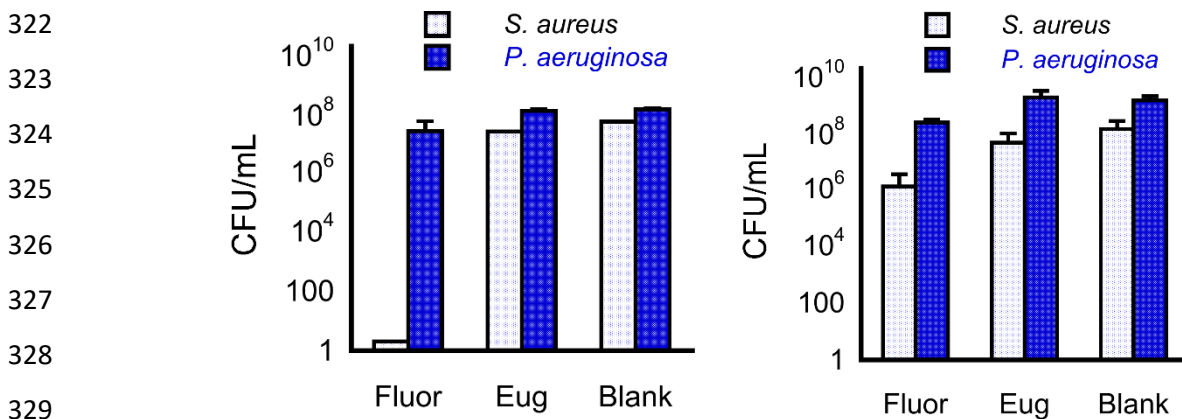


Fig. 3 Representative SEM images of cotton fibers: left image: untreated, central image: **Fabric A**, right image: **Fabric B**

3.3. Antimicrobial assays

309 The numbers of surviving colonies were quantified by plating the sample on agar plates (**Figure**
 310 **4**). An additional set of experiments was carried out to test if antibiotic leaching from the fabric
 311 was occurring and could be responsible for the observed antimicrobial activity (**Figure 4**).
 312 Firstly, we compared the activity of both fabrics for *S. aureus* (**Figure 4**). Only a slight
 313 bactericidal effect was observed for **Fabric A**. In contrast, **Fabric B** presented an excellent
 314 bactericidal performance for *S. aureus*, with a decrease of 7 log units in the concentration of
 315 the bacteria. Moreover, as it can be seen for the most active antimicrobial agent,
 316 fluoroquinolone (**Fabric B**), the effect of preincubation with the supernatant from the fabrics

317 does not reach the extent of the antimicrobial activity seen for *S. aureus* (**Figure 4**). This result
318 confirms the covalent attachment, which prevents leaching of the antibiotic from the textile, so
319 free detached fluoroquinolone is not responsible for the observed antimicrobial activity. A
320 plausible explanation for the antibacterial activity observed in our materials lies in the direct
321 contact between the surface of the textile and the bacteria in suspension.

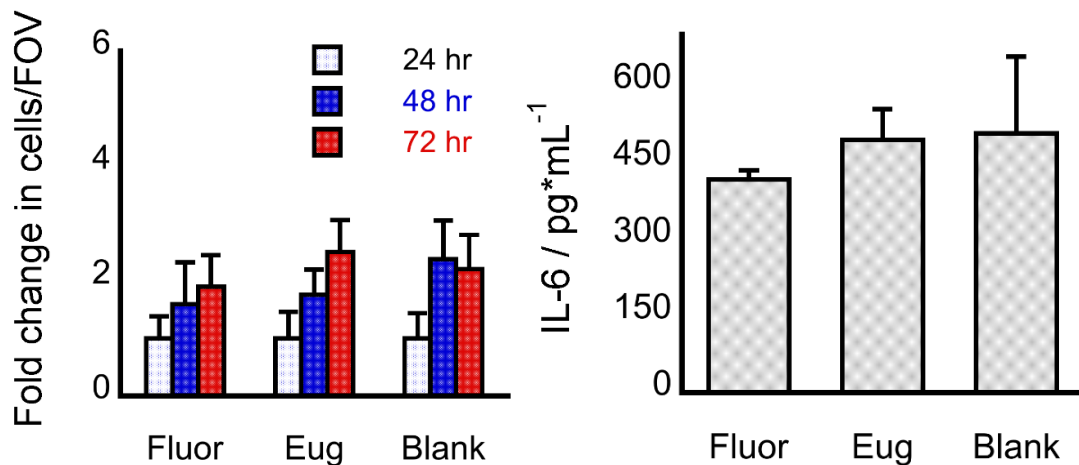


330 **Fig. 4. Left:** Surviving bacteria colonies after the incubation with *P. aeruginosa* and *S. aureus*
331 for 18h, see experimental, for: fabrics without antibiotics (blank), or those modified with
332 fluoroquinolone (Fluor) and eugenol (Eug). **Right:** Surviving bacteria colonies after incubation
333 of the bacteria inoculum in supernatant of presoaked fabrics with and without the antibiotics.
334 Values reported correspond to the standard deviation from the mean derived from 3 independent
335 experiments.

336

337 3.4. Biocompatibility and cell proliferation studies

338 *In vitro* studies were performed using human dermal skin fibroblasts to evaluate
339 biocompatibility and proliferation when cells are in contact with the fabrics. The results show
340 that the fabrics did not affect the proliferation profile of the cells (**Figure 5**), suggesting that
341 anchoring the antibiotic to the fabric does not lead to toxic side effects for cells in culture.
342 Confirming this, a LIVE/DEAD™ assay indicated that cell viability after 72 hours of incubation
343 in the presence of the fabrics was >95% in all cases. In addition, *in vivo* experiments carried
344 out in a murine model for non-healing wounds indicate no increase in IL-6 levels when the
345 fabric was put in contact with the wound (**Figure 5**).



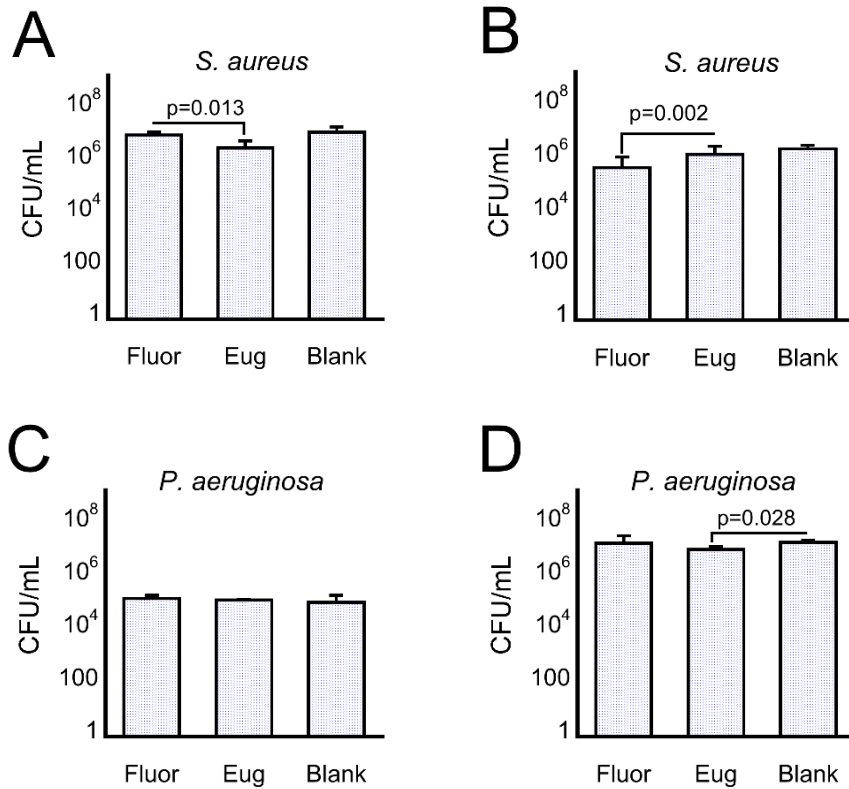
346
 347 **Fig. 5 Left:** Number of human skin fibroblasts per field of view (FOV) measured at different
 348 time points after seeding. The fabrics were placed in contact with the cells and only removed
 349 for capturing the images. Numbers reported correspond to the average of 3 independent
 350 samples. **Right:** Interleukin-6 (IL-6) levels for murine skin tissue wound beds homogenized
 351 after implantation of the fabric for 24h (n=4). Error bars correspond to the standard deviation
 352 from the mean.

353

354 3.5. Antibiofilm assays

355 Formation of biofilm is a survival strategy for bacteria to adapt to their environment (Irie et al.
 356 2012; Paharik et al. 2016). Under the protection of biofilm, microbial cells become tolerant and
 357 resistant to antibiotics and immune responses, which increase the difficulty for clinical
 358 treatments (Grupta et al. 2016; Katoona et al. 2018 (<https://www.heliyon.com/article/e01067/>)).
 359 Therefore, we studied the effectiveness of our treated fabrics on preventing and treating
 360 biofilms for *S. aureus* and *P. aeruginosa*. For *S. aureus* the fabrics containing eugenol showed
 361 a statistically lower number of survival bacteria in the prevention assay when compared to the
 362 fluoroquinolone group (**Figure 6A**). Meanwhile, the fluoroquinolone containing fabric was
 363 able to reduce the bacterial population in the biofilm form for *S. aureus* (**Figure 6B**). Thus,
 364 fluoroquinolone based **Fabric B** acts not only on the planktonic form of *S. aureus* strains but
 365 also on preformed *S. aureus* biofilms. As per the assays carried out for *P. aeruginosa*, no effect
 366 on preventing the biofilm formation was seen for any of the fabrics (**Figure 6C**), while only the
 367 eugenol containing fabric showed a lower bacterial population when acting on formed biofilm
 368 (**Figure 6D**).

369



370

371 **Fig. 6** Effect of antibiotic modification on the bacterial colony survival for *S. aureus* (A & B)
372 and *P. aeruginosa* (C & D) biofilms. The assays were carried out measuring the potency of the
373 fabrics to prevent the biofilm formation (A & C) as well as to assess their ability to kill bacteria
374 within a preformed biofilm (B & D). Values reported correspond to the average of 3
375 independent measurements, and error bars are the standard deviation from the mean (y-axis is
376 in log-scale). P values in the plots were calculated from t-Student test (two tailed).

377

378 4. Conclusion

379 In summary, new modified cotton fabrics were prepared through the covalent link of functional
380 bioactive molecules, such as eugenol and fluoroquinolone derivatives, on the surface of cotton
381 fabrics. Antibacterial tests performed with **Fabric A** coated with eugenol derivative showed no
382 antibacterial activity against planktonic forms of *S. aureus* and *P. aeruginosa*. However, **Fabric**
383 **B** coated with fluoroquinolone presented excellent antimicrobial activity with a decrease of 7
384 log units for the *S. aureus* strain. Similarly, the fluoroquinolone containing fabric was able to
385 significantly reduce preformed *S. aureus* biofilms, while **Fabric A** was the most active in
386 reducing *P. aeruginosa* biofilms. Moreover, **Fabric A** prevented to some extent *S. aureus*
387 biofilm formation. Incubation of the bacteria inoculum in supernatant of presoaked **Fabric B**
388 indicates no biocidal effect of the textile, which is indicative of no leaching of the

389 fluoroquinolone; similar results were observed for the less active eugenol modified fabric.
390 These covalently linked microbicidal agents do not leach into the surroundings of the textile,
391 so the probability of microorganisms developing resistance to them is small. Moreover, *in vitro*
392 and *in vivo* assays showed good biocompatibility of the fabrics. Therefore, these antimicrobial
393 textiles can be used, for example, for clothing, in hospital linen, in surgical masks, caps, and
394 gowns, as well as for wound healing, particularly in bandages or gauzes.

395

396 **Supplementary material**

397 Supplementary material is available. Copies of NMR, IR, HRMS spectra and compound
398 characterization are enclosed.

399

400 **Acknowledgements**

401 Financial support for this work was provided by the Spanish Ministerio de Ciencia, Innovación
402 y Universidades (Grants CTQ2014-53662-P, RTI2018-097853-B-I00 and 2016-81797-REDC)
403 and by Generalitat de Catalunya (2017 SGR 00465). EIA and EJS thanks to the Canadian
404 Institutes of Health Research (CIHR) for financial support. EIA also thanks the support of
405 NSERC through the Discovery Grant program. AEK is appreciative to University of Ottawa
406 for an Undergraduate Research Opportunity Award. CL is thankful for the Queen Elizabeth II
407 Graduate Scholarship in Science and Technology.

408

409 **References:**

410 Abramiuc D, Ciobanu L, Muresan R, Chiosac M, Muresan A (2013) Antibacterial finishing of
411 cotton fabrics using biologically active natural compounds. *Fibers and Polymers* 14:1826-1833.

412 Aldred J K, Kerns R J, Osheroff N (2014) Mechanism of quinolone action and resistance.
413 *Biochemistry* 53:1565-1574.

414 Benecia F, Courreges M C (2000) In vitro and in vivo activity of eugenol on human herpesvirus.
415 *Phytother. Res.* 14: 495-500.

416 Blaszyk M, Holley R A (1998) Interaction of monolaurin, eugenol and sodium citrate on growth
417 of common meat spoilage and pathogenic organisms. *Int. J. Food. Microbiol.* 39:175-183.

418 Dondoni A (2008) The emergence of thiol-ene coupling as a clickprocess for materials and
419 bioorganic chemistry. *Angew. Chem. Int. Ed.* 47:8995-8997.

420 Dong C, He P, Lu, Z, Wang, S, Sui S, Liu J, Zhang L, Zhu P (2018) Preparation and properties
421 of cotton fabrics treated with a novel antimicrobial and flame retardant containing triazine and
422 phosphorous components. *J. Therm. Anal. Calorim.* 131: 1079-1087.

- 423 Gargoubi S, Tolouei R, Chevallier P, Levesque L, Iadhari N, Boudokhabe C, Mantovani D
424 (2016) Enhancing the functionality of cotton fabric by physical and chemical pre-treatments: A
425 comparative study. *Carbohydrate Polymers* 147:28-36.
- 426 Gupta P, Sarkar S, Das B, Bhattacharjee, S, Tribedi P (2016) Biofilm, pathogenesis and
427 prevention--a journey to break the wall: a review. *Arch. Microbiol.* 198(1):1-15
- 428 Gutarowska B, Machnowski W, Kowzowicz L (2013) Antimicrobial activity of textiles with
429 selected dyes and finishing agents used in the textile industry. *Fiber. Polym.* 14:415-422.
- 430 Hong K H (2014) Preparation and properties of multifunctional cotton fabrics treated by
431 phenolic acids. *Cellulose* 21:2111-2117.
- 432 Hsu B B, Klivanov A M (2011) Light-Activated Covalent Coating of Cotton with Bactericidal
433 Hydrophobic Polycations. *Biomacromolecules* 12:6-9.
- 434 Irie Y, Borlee B R, O'Connor J R, Hill P J, Harwood C S, Wozniak D J, Parsek M R (2012)
435 Self-produced exopolysaccharide is a signal that stimulates biofilm formation in *Pseudomonas*
436 *aeruginosa*. *Proc. Natl. Acad. Sci.* 109: 20632-20636.
- 437 Jiang Z, Qiao M, Ren X, Zhu P., Huang T-Z (2017) Preparation of antibacterial cellulose with
438 s-triazine-based quaternarized *N*-halamine. *J. Appl. Polym. Sci.* 134:n/a.
- 439 Kalembe D, Kunicka A (2003) Antibacterial and antifungal properties of essential oils. *Curr.*
440 *Med. Chem.* 10:813-829.
- 441 Khatoona Z, McTiernana C D, Suuronena E J, Mahb T-F, Alarcon E I (2018) Bacterial biofilm
442 formation on implantable devices and approaches to its treatment and prevention. *Heliyon*
443 4:e01067.
- 444 Klivanov A M (2007) Permanently microbicidal materials coatings. *J. Mater. Chem.* 17: 2479-
445 2482.
- 446 Koga H, Ittoh A, Murayama S, Suzue S, Irikura T (1980) Structure-activity relationships of
447 antibacterial 6,7- and 7,8-disubstituted 1-alkyl-1,4-dihydro-4-oxoquinoline-3-carboxylic acids.
448 *J. Med Chem.* 23:1358-1363.
- 449 Koga H, Tokunaga E, Hidaka M, Umemura Y, Saito T, Isogai A, Kitaoka T (2010)
450 Topochemical synthesis and catalysis of metal nanoparticles exposed on crystalline cellulose
451 nanofibers. *Chem. Commun.* 46:8567–8569.
- 452 Koh E, Hong K H (2014) Gallnut extract-treated wool and cotton for developing green
453 functional textiles. *Dyes Pigments* 103:222-227.
- 454 Lenardão E J, Jacob R G, Mesquita K D, Lara R G, Webber R, Martínez D M, Savegnago L,
455 Mendes S R, Alves D, Perin G (2013) Glycerol as a promoting and recyclable medium for
456 catalyst-free synthesis of linear thioethers: new antioxidants from eugenol. *Green Chem. Lett.*
457 *Rev.* 2013, 6:269-276.
- 458 Leyva S, Leyva E (2008) Fluoroquinolonas. Mecanismos de acción y resistencia, estructura,
459 síntesis y reacciones fisicoquímicas importantes para propiedades medicinales. *Bol. Soc. Quim.*
460 *Méx.* 2:1-13.

- 461 Lin J, Murthy S J, Olsen B D, Gleason K K, Klivanov A M (2003) Making thin polymeric
462 materials, including fabrics, microbicidal and also water-repellent. *Biotechnol. Lett.* 25:1661-
463 1665.
- 464 Liu K, Tian Y, Jiang L (2013) Bio-inspired superoleophobic and smart materials: Design,
465 fabrication, and application. *Progress in Materials Science* 58:503-564.
- 466 Montagut A M, Gálvez E, Shafir, A, Sebastián R M, Vallribera A (2017) Triarylmethane dyes
467 for artificial repellent cotton fibers. *Chem. Eur. J.* 23:3810-3814.
- 468 Öktem T (2003) Surface treatment of cotton fabrics with chitosan *Color. Technol.* 119:241-
469 246.
- 470 Paharik A E, Horswill A R (2016) The staphylococcal biofilm: adhesins, regulation, and host
471 response. *Microbiol. Spectr.* 4(2):1-27.
- 472 Pinho E, Henriques M, Oliveira R, Dias A, Soares G (2010) Development of biofunctional
473 textiles by the application of resveratrol to cotton, bamboo, and silk. *Fiber. Polym.* 11:271-276.
- 474 Ristić T, Zemljič L F, Novak M, Kunčič M K, Sonjak S, Cimerman N G, Strnad G (2011)
475 Science against microbial pathogens: communicating current research and technological
476 advances, Méndez-Vives, Formatex Research Center, Spain.
- 477 Rojo L, Barcenilla J M, Vázquez B, Gonzalez R, Román J S (2008) From natural products to
478 polymeric derivatives of “eugenol”: A new approach for preparation of dental composites and
479 orthopedic bone cements. *Biomacromolecules* 9:2530-2535.
- 480 Salabert J, Sebastián R M, Vallribera A (2015) Anthraquinone dyes for superhydrophobic
481 cotton. *Chem. Commun.* 51:14251-14251.
482
- 483 Salama A A A, Koth R M, Shaker R N (2015) Effect of treatment durability and coloration of
484 coated cotton fabrics on antibacterial, UV-blocking, healing and anti-inflammatory properties.
485 *J. Chem. Pharm. Res.* 7:181-193.
- 486 Shahidi S, Aslan N, Ghoranneviss M, Korachi M (2014) Effect of thymol on the antibacterial
487 efficiency of plasma-treated cotton fabric. *Cellulose* 21:1933-1943.
- 488 Shahidi S, Wiener J (2012). *Antimicrobial agents* Ed. V. Bobbarala InTechOpen, p. 387-406.
- 489 Simoncic B, Tomsic B (2010) Structures of novel antimicrobial agents for textiles - A review.
490 *Text. Res. J.* 80:1721-1737.
- 491 Soler R, Salabert J, Sebastián R M, Vallribera A, Roma N, Ricart S, Molins E (2011) Highly
492 hydrophobic polyfluorinated azo dyes grafted on surfaces. *Chem. Comm.* 47:2889-2891.
- 493 Song L, Baney R H (2016) Antibacterial evaluation of cotton textile treated by trialkoxysilane
494 compounds with antimicrobial moiety. *Text. Res. J.* 81:504-511.
- 495 Sun G, Xu X, Bickett J R, Williams J F (2001) Durable and regenerable antibacterial finishing
496 of fabrics with a new hydantoin derivative. *Ind. Eng. Chem. Res.* 40:1016-1021.

- 497 Vazquez B I, Fente C, Franco C M, Vazquez M J, Cepeda A (2001) Inhibitory effects of eugenol
498 and thymol on *Penicillium citrinum* strains in culture media and cheese. *Int. J. Food Microbiol.*
499 *67*:157-163.
- 500 Yang K, Clark M, Lewis, D M (2018) Synthesis of a di(*p*-sulphophenoxy)-*s*- triazine reactive
501 dye and its application in wool fabric ink-jet printing. *Colora. Technol.*
502 <https://doi.org/10.1111/cote.12388>
- 503 Xu Y, Xue M, Li J, Zhang L, Cui Y (2010) Synthesis of a cellulose xanthate supported
504 palladium(0) complex and its catalytic behavior in the Heck reaction. *React. Kinet. Mech. Catal.*
505 *100*:347-353.
- 506

507 **Highlights**

- 508 • Eugenol and fluoroquinolone derivatives have been covalently attached onto the surface
509 of cotton fabrics.
- 510 • Fluoroquinolone containing presented antimicrobial activity decreasing 7 log units for
511 the *S. aureus* strain and reduce significantly preformed biofilms.
- 512 • The evaluation of the *in vitro* biocompatibility showed no toxic effects in human skin
513 cells.
- 514 • The modified fabrics did not increase the levels of IL-6 in a full-thickness wound model
515 in mice.